ELSEVIER

Journal of Photochemistry and Photobiology A: Chemistry 129 (1999) 147–156

Journal of Photochemistry and Photobiology A:Chemistry

www.elsevier.nl/locate/jphotochem

Polarization-induced intramolecular photodimerization in uniaxially stretched poly(methyl methacrylate)

Takahiro Okamoto [1], Yuji Imamura, Osamu Urakawa [2], Qui Tran-Cong *

Department of Polymer Science and Engineering, Kyoto Institute of Technology, Matsugasaki, Kyoto 606-0085, Japan

Received 28 June 1999; received in revised form 4 September 1999; accepted 10 September 1999

Abstract

Intramolecular photodimerization of the diphant-type molecule 9-hydroxymethyl-10-{(1-naphthylmethoxy) methyl} anthracene (HNMA) was induced in the glassy state of poly(methyl methacrylate) (PMMA) by irradiation with linearly polarized light. The selectivity of the reaction was quantitatively evaluated by measuring the two polarized absorbance components of HNMA in the directions parallel and perpendicular to the polarization (E) of the exciting light. Both the reaction kinetics and the extremely slow reorientation dynamics of HNMA in the glassy matrix were obtained respectively by monitoring the time-dependence of the total absorbance and the decay of the dichroic absorption using the annealing-after-irradiation method. These kinetic data are taken along the directions parallel and perpendicular to the stretching direction (S) of the sample by changing the relative orientation of (E) with respect to (S). The anisotropy of the reaction and the transport coefficients in uniaxially oriented PMMA are discussed in conjunction with the rotational diffusion-controlled reaction model proposed recently. ©1999 Published by Elsevier Science S.A. All rights reserved.

Keywords: Polarization-induced photochemical reaction; Uniaxially orientated poly(methyl methacrylate); Photodimerization; Anthracene; Anisotropic reorientation relaxation

1. Introduction

Transport phenomena in anisotropic media have been of great interest because of their relations to the regulation of biomembrane functionality [1] as well as optical response of oriented organic systems such as liquid crystals [2]. The transport processes such as translational or reorientational diffusion in polymeric systems, particularly in their glassy state, are not easily measurable because the characteristic times involving in the process are much longer than the time scale of our daily life. Recently, the experimental techniques for observing extremely slow reorientational diffusion become indispensable to elucidate the molecular mechanism behind the instability of nonlinear optical properties of materials composed of guest dyes dispersed in host polymer matrices [3].

We have demonstrated that by irradiating photochromic molecules dispersed in polymers with linearly polarized light, the orientational distribution of the reaction can be induced in the glassy state of polymer matrix [4]. As a consequence, the optical anisotropy of the polymer matrix can be generated and controlled by using polarized light [5]. According to the rotational diffusion-controlled reaction model proposed recently [6], the time-evolution of the optical anisotropy generated upon irradiation with linearly polarized light is governed by two factors: the reaction rate k and the reorientational diffusion coefficient D. The former is directly obtained from the time-dependence of the total absorbance whereas the latter can be extracted from the decay of the reaction selectivity observed in the annealing-after-irradiation experiments [7]. Though the mean-field reaction kinetics was assumed, for simplicity, in the above-mentioned reaction-diffusion model, it has been used succesfully to explain the time-dependence of the optical anisotropy generated in the glassy state of isotropic poly(methyl methacrylate) (PMMA) [8], in PMMA films aged under different conditions [9] and in polystyrene/poly(vinyl methyl ether) miscible blends [10].

In this paper, the intramolecular photodimerization of 9-hydroxymethyl-10-{(1-naphthylmethoxy) methyl} anthracene (HNMA) was investigated in a uniaxially oriented PMMA matrix. Both the reaction kinetics as well as the

---

* Corresponding author.

E-mail address: qui@ipc.kit.ac.jp (Q. Tran-Cong)

[1] Present address: Japan Synthetic Rubbers Inc., Yokkaichi, Mie, Japan.

[2] Permanent address: Department of Macromolecular Science, Osaka University, Toyonaka, Osaka 560-0043, Japan.

PII: S1010-6030(99)00189-6

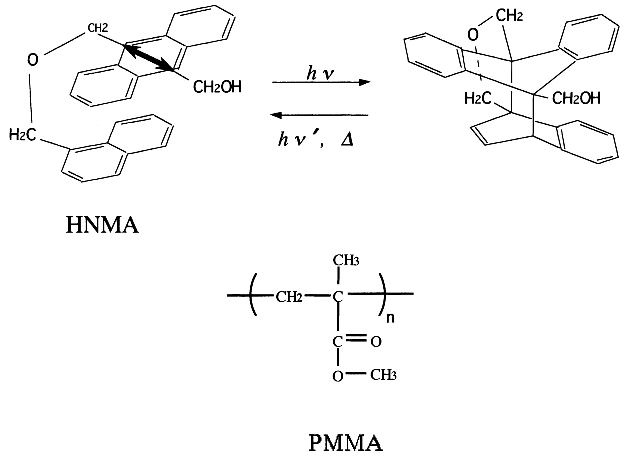

Fig. 1. Intramolecular photodimerization of 9-hydroxymethyl-10-{(1-naphthylmethoxy) methyl} anthracene (HNMA) and the chemical structure of poly(methyl methacrylate) (PMMA). The arrow on the anthracene moieties indicates the absorption transition moment of the molecule.

reorientational dynamics of HNMA were separately observed in the directions parallel and perpendicular to the stretching direction (S) of the PMMA matrix by varying the direction of the polarization (E) of the exciting light with respect to (S). The temperature dependence of these transport coefficients was observed together with the selectivity of the reaction under various experimental conditions. Finally, the behavior of the reorientation dynamics of HNMA in anisotropic media was discussed in conjunction to the diffusion-controlled reaction model proposed recently.

2. Experimental section

2.1. Samples

9-hydroxymethyl-10-{(1-naphthylmethoxy) methyl} anthracene (HNMA) was synthesized and purified according to the procedure reported previously [4,11]. Poly(methyl methacrylate) (PMMA) was purchased from Wako Chemicals (Japan) and was purified by using tetrahydrofuran (THF) as good solvent and methanol as non-solvent. The chemical structure of HNMA and PMMA is shown in Fig. 1. It is worth noting that the direction of the absorption transition moment of the anthracene moieties of HNMA is oriented along the 9- and 10-positions of the molecule. HNMA was incorporated into PMMA film by casting benzene solutions of PMMA containing an appropriate amount of HNMA. The concentration of HNMA in PMMA films was fixed at 10^{-3} M. PMMA/HNMA films with the size $13 \times 9 \times 0.2\,\mathrm{mm}^3$ were dried at 130°C in vacuo over 60 h and were subsequently sealed between two quartz plates with a 0.2 mm spacer to avoid the contact with air. Finally, the samples were annealed at 170°C in vacuo in 10 h prior to the experiments.

2.2. Procedure of elongation

A PMMA film containing HNMA with two ends fixed to an extender was dipped into silicon oil thermostated at 120°C which is located at +15°C above the glass transition temperature (T_g) of the PMMA matrix. After 10 min, the time required for thermal equilibration, the film was uniaxially stretched inside the silicon oil with the rate 1 mm/min. As its length achieves the desired elongation ratio α defined as, $\alpha = (L/L_0)$ the stretched sample was quenched into another bath of silicon oil kept at 30°C in 10 min. Here, L_0 and L are respectively, the lengths of the PMMA film before and after elongation. Subsequently, the stretched sample was taken out of the oil bath, wiped with *n*-hexane to remove the residual oil at the surface and was kept at room temperature in 16 h with both ends fixed by adhesive on a quartz plate prior to the experiments. This procedure is necessary to equilize the thermal history of all the samples to avoid the physical aging effects [9]. Isotropic (unstretched) samples prepared with the similar procedure were also used for comparison. It is worth noting that after the elongation process, both the stretched and unstretched samples have the same thickness 0.2 mm. For all the data described hereafter, samples with the elongation ratio $\alpha = 1$ (unstretched) and 3.0 (stretched) were used throughout this study.

2.3. Irradiation experiments

PMMA films doped with HNMA were irradiated along the two directions under which the polarization direction (E) of the exciting light is parallel and perpendicular to the elongational direction (S) of the sample. For convenience, these are named hereafter as *parallel* ($E \parallel S$) and *perpendicular* ($E \perp S$) irradiation. For each direction of irradiation, the absorbance of the anthracene moieties of HNMA was monitored along the directions parallel and perpendicular to the polarization (E). A PMMA film containing HNMA was placed in a brass heating block thermostated with a precision of ±0.5°C by using a temperature controller (Ohkura Electrics Inc., Model EC-5600). The unpolarized light from a high-pressure Hg-Xe lamp (250 W, Ushio Electrics Inc.) was converted into linearly polarized light by a UV polarizer (Polaroid, Model HNP'B) placed in the front of the sample. To avoid the photodissociation of anthracene photodimer, a sharp-cut filter (Corning, SC-052) was used to extract the UV light with the wavelengths longer than 300 nm for excitation. The intensity at 365 nm was adjusted at $0.25\,\mathrm{mW/cm}^2$.

2.4. Measurements and data analysis

After irradiation with linearly polarized light over a fixed period of time, the two polarized components of the absorbance of HNMA in the film were measured along the two directions with respect to the polarization (E) of the exciting light as illustrated in the coordinate system of Fig. 2.

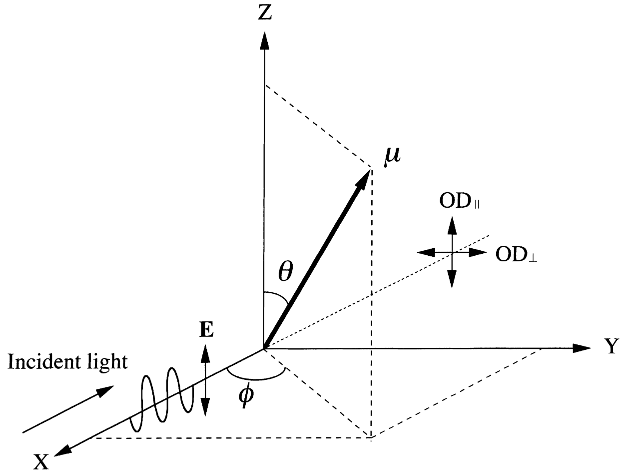

Fig. 2. The coordinate system for measuring the dichroic absorption of HNMA. μ is the absorption transition moment of the anthracene moieties of HNMA and E is the electric field vector of the incident polarized light.

The following quantities were used to evaluate the reaction kinetics as well as the reorientational relaxation of HNMA in the PMMA matrix.

(a) The selectivity of the reaction (η):

$$\eta(t) = \frac{[\mathrm{OD}_{\perp}(t) - \mathrm{OD}_{\parallel}(t)]}{\mathrm{OD}_0} \times 10^2 \tag{1}$$

(b) The total absorbance ($\mathrm{OD}_{\mathrm{tot}}$):

$$\mathrm{OD}_{\mathrm{tot}}(t) = [\mathrm{OD}_{||}(t) + 2\mathrm{OD}_{\perp}(t)] \tag{2}$$

Here, $\mathrm{OD}_0 = \mathrm{OD}_{\mathrm{tot}}(t=0)$ is the initial absorbance at 394.5 nm of the anthracene moieties of HNMA measured before irradiation. $\mathrm{OD}_{\perp}$(t) and $\mathrm{OD}_{||}$(t) are the two polarized absorbance components observed in the directions perpendicular and parallel to (E) after t min of irradiation. Physically, the reaction selectivity $\eta(t)$ indicates the extent of the optical anisotropy generated in the sample whereas the total absorbance $\mathrm{OD}_{\mathrm{tot}}(t)$ corresponds to the absorption obtained by irradiation with *unpolarized* light.

According to the rotational diffusion-controlled reaction model [6] outlined below, the selectivity $\eta(t)$ is a function of (k/D) where k and D are respectively the reaction rate and the rotational diffusion coefficient of HNMA. The intramolecular photodimerization kinetics of HNMA under irradiation with linearly polarized light can be obtained by fitting the data of $\mathrm{OD}_{\mathrm{tot}}(t)$ to an appropriate model function. On the other hand, the extremely slow reorientation of HNMA in uniaxially oriented PMMA was observed by following the decay of the selectivity $\eta(t)$ with annealing time at a constant temperature. Analysis of $\mathrm{OD}_{\mathrm{tot}}(t)$ and $\eta(t)$ provides the kinetic parameters of both the reaction and the reorientational relaxation of HNMA in oriented PMMA matrix.

2.5. Outline of the rotational diffusion-controlled reaction model

The intramolecular photodimerization induced by irradiation with linearly polarized light can be described by the following rotational diffusion-controlled reaction [6]:

$$\frac{\partial W(\theta,t)}{\partial t} = D\frac{1}{\sin\theta}\frac{\partial}{\partial\theta}\sin\theta\left[\frac{\partial W(\theta,t)}{\partial\theta}\right] - k\cos^2\theta\, W(\theta,t) \tag{3}$$

where $W(\theta,\ t)$ is the transition probability for finding the absorption dipole of the anthracene moieties of HNMA at an angle θ and time t, D the rotational diffusion coefficient, k the reaction rate of HNMA.

For the sake of simplicity, the mean-field kinetics was assumed for the reaction term in Eq. (3). The two polarized absorbance components $\mathrm{OD}_{\perp}(t)$ and $\mathrm{OD}_{||}$(t) of HNMA are related to the solution of Eq. (3) by

$$\mathrm{OD}_{||}(t) = \int_0^{2\pi}\int_0^{\pi} \mu^2\cos^2\theta\ W(\theta,\phi,t)\sin\theta\,\mathrm{d}\theta\,\mathrm{d}\phi$$

$$\mathrm{OD}_{\perp}(t) = \int_0^{2\pi}\int_0^{\pi} \mu^2\sin^2\theta\sin^2\phi\ W(\theta,\phi,t)\sin\theta\,\mathrm{d}\theta\,\mathrm{d}\phi$$

Here the transition probability $W(\theta,\ \phi,\ t)$ was taken as $W(\theta,\ t)$ because of its symmetry with respect to the Z-axis of the spherical coordinate.

It was found that there exist two cases for the reaction selectivity of HNMA:

Case A: where the reaction yield Φ is small. Namely, the concentration of the reacted HNMA is much smaller than the initial concentration. Under this particular condition, the dichroism defined as

$$\Delta(t) = \mathrm{OD}_0\eta(t) = [\mathrm{OD}_{\perp}(t) - \mathrm{OD}_{||}(t)] \tag{4}$$

is related to the reaction rate k and the rotational diffusion coefficient D by

$$\Delta(t) = \Delta_{\max}(1 - \mathrm{e}^{-t/\tau}) \tag{5}$$

where

$$\Delta_{\max} \cong \frac{2k}{15(6D + (k/5))} \tag{6}$$

and

$$\tau \cong \frac{1}{6D + k/5} \tag{7}$$

OD_0 in Eq. (4) is the absorbance of HNMA measured before irradiation ($t=0$). The symbol $\cong$ arises from the approximation of neglecting the higher order terms in the final results expressed by infinite continued fractions [12].

(b) *Case* B: where the reaction yield Φ is high and the change in the concentration of HNMA is no longer negligible. For the particular case $\Phi = 1/2$, the dichroism is given by

$$\Delta(t) = \Delta_{\max}\frac{T}{(T-\tau)}(\mathrm{e}^{-t/T} - \mathrm{e}^{-t/\tau}) \qquad (8)$$

Here, the characteristic time $T \cong 1/k$ arises from the concentration depletion induced by the high yield of the reaction. Eq. (8) suggests that the reaction selectivity will pass through a maximum before it disappears at long irradiation time. As seen below, the intramolecular photodimerization of HNMA in glassy PMMA described in this work belongs to the Case A.

3. Results and discussion

3.1. Selectivity of the photodimerization in glassy PMMA matrix

The irradiation time dependence of the two components of the polarized absorbance and the reaction selectivity $\eta(t)$ of HNMA in PMMA observed at 40°C is shown in Fig. 3 for the three experimental conditions: in isotropic PMMA matrix (a), parallel (b) and perpendicular irradiation (c) in a uniaxially stretched PMMA film with $\alpha = 3$. The absorbance component observed in the direction perpendicular with the exciting polarization (E) is always larger than the parallel direction for all conditions, indicating that the intramolecular photodimerization of HNMA proceeds selectively under irradiation with linearly polarized light. Furthermore, the reaction selectivity $\eta(t)$ increases with increasing irradiation time and then approaches the limiting value whose magnitude depends strongly on the experimental temperature. These results reveal the time-evolution for the forming process of the optical anisotropy in these PMMA films. It is worth noting that for the case $\alpha = 3$, the difference in the initial absorbance OD_0 obtained by the parallel and perpendicular irradiation is less than 3%, indicating that the orientation of HNMA is almost unaffected under the stretching conditions of this experiment. As indicated by the solid curve in Fig. 3, the rise of $\eta(t)$ is almost expressible by an exponential function of irradiation time as predicted by the model. The variation of $\eta_{\max}$ with the experimental temperature is shown in Fig. 4 for these three conditions. It was found that, though the difference in $\eta_{\max}$ between the unstretched and the uniaxially oriented PMMA films obtained by the parallel irradiation is not significant, $\eta_{\max}$ resulting from the perpendicular irradiation is much higher than the case of parallel irradiation. The experimental data shown in Fig. 4 are seemingly different from the preliminary result illustrated in Fig. 3 of the previous report [13]. The reason responsible for this inconsistency originates from the non-unified thermal histories prior to measurements of the oriented samples in the previous experiments. The limiting anisotropy decreases as temperature increases for all three cases and tends to disappear as the experimental temperature approaches the glass transition temperature (T_g) of the PMMA matrix. This result reveals the significant contribution of the orientational relaxation of HNMA to the forming optical anisotropy of the samples. As described later, the behavior of HNMA observed in Figs. 3 and 4 for these three cases can be explained by using the reaction-diffusion model with the kinetic parameters obtained from both the intramolecular photodimerization and the reorientational relaxation of HNMA.

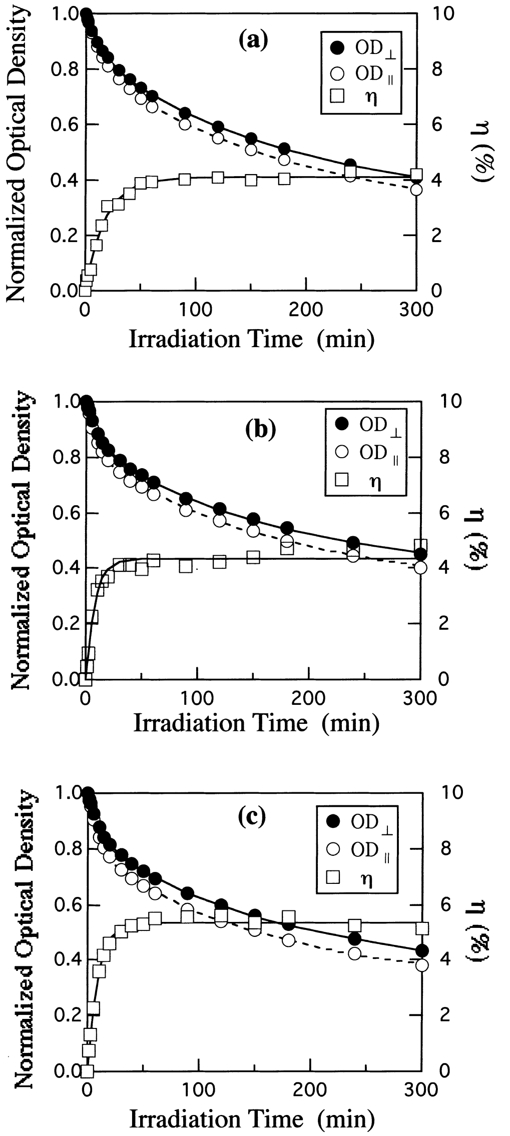

Fig. 3. Irradiation-time dependence of the two components of the polarized absorbance and the reaction selectivity observed for HNMA in: (a) isotropic PMMA; (b) parallel irradiation (E ∥ S) and (c) perpendicular irradiation (E ⊥ S). All the data were taken at 40°C. The elongation ratio α is 3.0.

3.2. Photodimerization kinetics in uniaxially oriented glassy PMMA

The reaction kinetics of HNMA in the unstretched (isotropic) and uniaxially stretched (anisotropic) PMMA

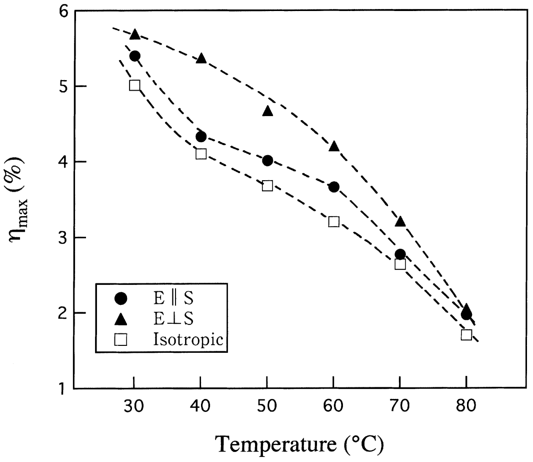

Fig. 4. Temperature dependence of the limiting selectivity of the reaction corresponding to the data shown in Fig. 3.

films was observed by monitoring the irradiation time-dependence of the total absorbance $OD_{tot}(t)$ defined in Eq. (2). Shown in Fig. 5 are the total absorbances of HNMA obtained under the three experimental conditions corresponding to those in Fig. 3. For convenience, the maximum magnitudes of the total absorbance were normalized to 3.0. The difference in the decay processes of these three cases is not significant for the elongation ratio $\alpha = 3$. To evaluate the reaction kinetics in a more quantitative way, $OD_{tot}(t)$ obtained in Fig. 5 was fitted to the following model function:

$$OD_{tot}(t) = F_f \exp(-k_f t) + F_s \exp(-k_s t) + B \qquad (9)$$

where k_f and k_s are respectively the reaction rates of the fast and slow processes with the corresponding fractions F_f and F_s. B is the baseline expressing the fraction of HNMA which cannot undergo photodimerization due to the suppression of HNMA conformational transitions in the regions with free-volumes much smaller than its size.

The reaction rates k_f and k_s can be interpreted as the rates of the intramolecular photodimerization in the regions with the free-volumes v_f satisfying the condition $v_f \gg v^*$ and $v_f \cong v^*$, respectively. Here, v^* is the critical free-volume required for the reaction. The fractions F_f and F_s correspond to the number of HNMA in these regions. The best fit obtained with the model function given by Eq. (9) is indicated by the solid line in Fig. 5. It should be noted that, as shown earlier [14], the so-called stretched exponential or the Kohlrausch–Williams–Watts (KWW) function [15,16] did not provide a good fit for the decay of absorbance over the whole range of experimental temperatures. Physically, the essential feature of the KWW model is that the sizes involving in the relaxation process change as the observation time increases. This particular behavior might not appropriately describe the relaxation behavior of HNMA in the inhomogeneous environments such as glassy polymers where there exists a free-volume distribution [17–20]. Shown in Figs. 6 and 7 are the temperature dependence of the slow and fast reaction rates k_f, k_s and their corresponding fractions F_f, F_s. The variation of the baseline B is also illustrated in Fig. 7(c). It was found that the fast reaction rate k_f is almost unchanged within the range of the experimental temperatures, whereas the slow reaction rate k_s slightly increases with temperature. k_f and k_s obtained for the isotropic and anisotropic samples do not exhibit significant difference. On the other hand, the two fractions F_f and F_s obtained under these three conditions increase with increasing temperature, whereas the baseline B, i.e. the fraction of the unreacted HNMA, decreases as the temperature approaches Tg of the PMMA matrix. From these kinetic data, it can be concluded that the difference in the reaction kinetics for the isotropic and anisotropic systems is not significant for the case $\alpha = 3.0$.

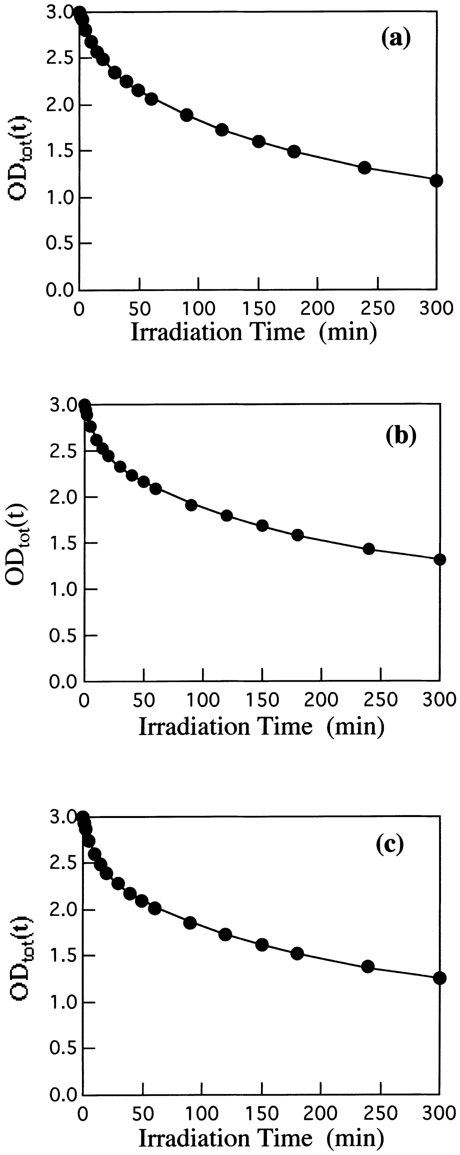

Fig. 5. Irradiation-time dependence of the total absorbance $OD_{tot}(t)$ obtained for HNMA in PMMA under the three conditions described in Fig. 3. (a) isotropic sample parallel (b) and perpendicular (c) irradiation for a uniaxially oriented sample.

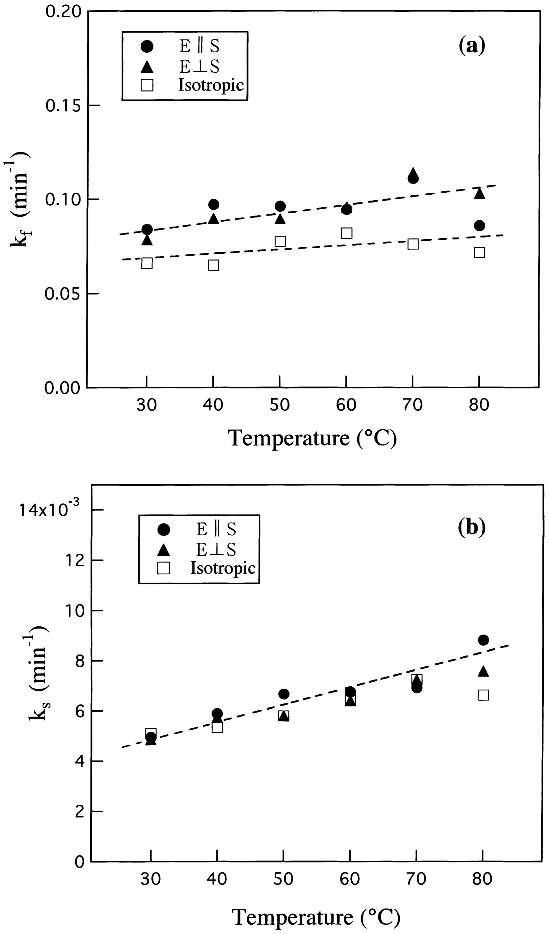

Fig. 6. Temperature dependence of the fast (a) and slow (b) rates of the photoisomerization of HNMA obtained in isotropic PMMA and by parallel, perpendicular irradiation for uniaxially stretched PMMA. The dotted lines are for eye-guidance.

3.3. Reorientational relaxation in uniaxially oriented PMMA matrix

In order to observe the reorientational relaxation process of HNMA in uniaxially elongated PMMA matrix, a stretched PMMA containing HNMA was first irradiated at 40°C over 90 min which is the time required for the reaction selectivity $\eta(t)$ to reach its maximum value $\eta_{\max}$. Subsequently, the sample was annealed in the dark at various temperatures while the variation of the reaction selectivity of HNMA was monitored with annealing time.

As an example, the reorientational relaxation of HNMA in PMMA obtained by the annealing-after-irradiation at 50°C is shown in Fig. 8 for the three cases: isotropic matrix, parallel (E ∥ S) and perpendicular (E ⊥ S) irradiation for a uniaxially oriented matrix. It is obvious that the decay process of $\eta(t)$ cannot be described by the stretched exponential function, but instead it can be well fitted to the sum of a fast and a slow exponential decay function given by

$$\eta(t) = R_\mathrm{f}\exp(-D_\mathrm{f}t) + R_\mathrm{s}\exp(-D_\mathrm{s}t) \qquad (10)$$

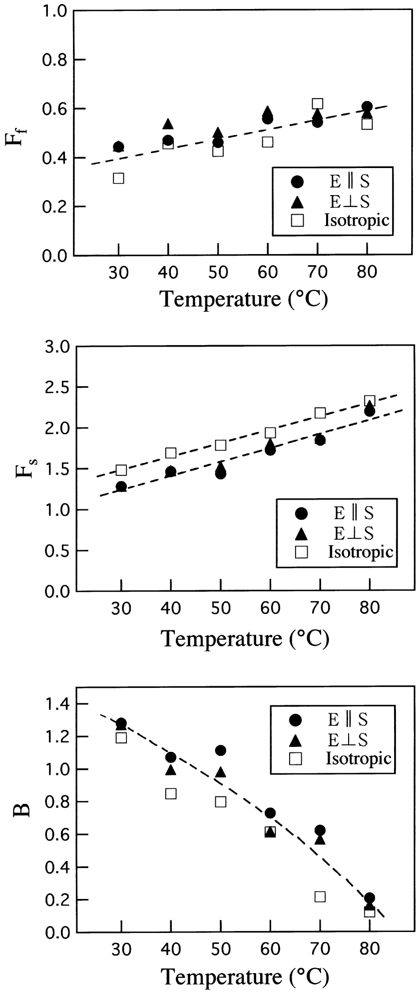

Fig. 7. Temperature dependence of the fractions F_f and F_s corresponding to the two photodimerization processes illustrated in Fig. 6 and of the baseline B for isotropic and uniaxially stretched PMMA matrices. The dotted lines are for eye-guidance.

Here D_f and D_s are respectively the reorientational relaxation rates of the fast and slow processes of HNMA. R_f and R_s are the corresponding fractions of these two processes.

It is worth noting that Eq. (10) does not contain a base line as Eq. (9) because the optical anisotropy arising from the reaction selectivity will eventually disappear at high temperature. The variation of the rates of the fast and the slow relaxation processes given in Eq. (10) is shown in Fig. 9 where D_f and D_s are plotted versus temperature. It was found from these results that for the fast process, the reorientational relaxation of HNMA in the isotropic sample seems to be faster than those in the uniaxially oriented PMMA, whereas the difference in D_f obtained by the parallel and perpendicular irradiation is not significant within the temperature range of the experiments. One of the reason responsible for this insignificance would be due to the decay process of $\eta(t)$ in the early stage of irradiation which is too fast to be determined with accuracy by conventional techniques. However, the difference in the reorientational relaxation of HNMA observed

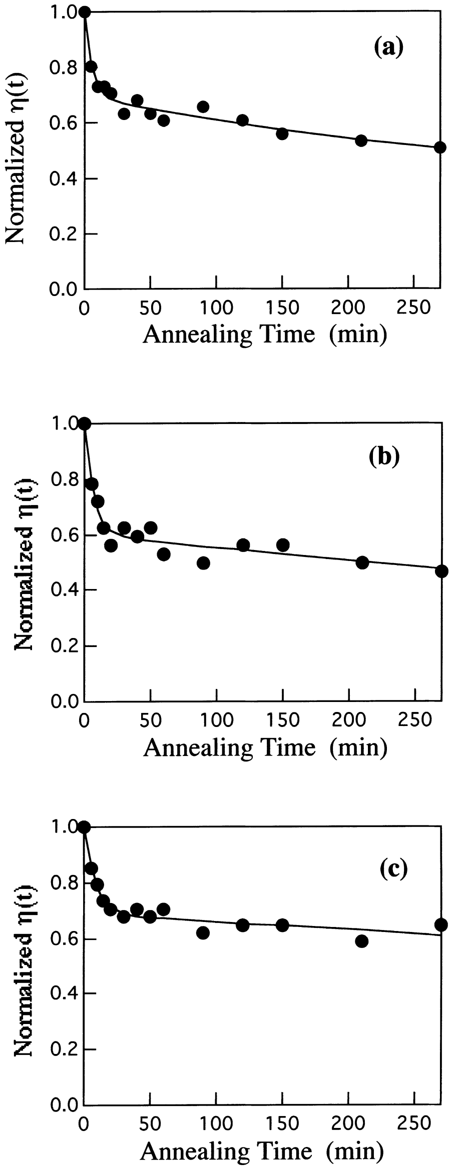

Fig. 8. Annealing-time dependence of the reaction selectivity of HNMA in PMMA under three conditions obtained at 50°C: (a) isotropic PMMA film; (b) parallel and (c) perpendicular irradiation for a uniaxially stretched PMMA film. The elongation ratio α is 3.0.

for these two cases of irradiation becomes significant for the slow decay process as shown in Fig. 9b. These data indicate that in uniaxially oriented PMMA, the reorientational relaxation of HNMA along the stretching direction is much faster than in the perpendicular direction. Namely, within the anisotropic (ellipsoidal) free-volumes formed by uniaxially stretched polymer chains around HNMA, the restriction imposed on the reorientational relaxation along the direction perpendicular to the stretching direction (the short axis of the ellipsoidal free-volumes) would be stronger than in the parallel direction (the long axis of the ellipsoidal free-volumes). Similar conclusions have been reached by several authors who have used forced Rayleigh scattering to measure the translational diffusion of small molecules in liquid crystals

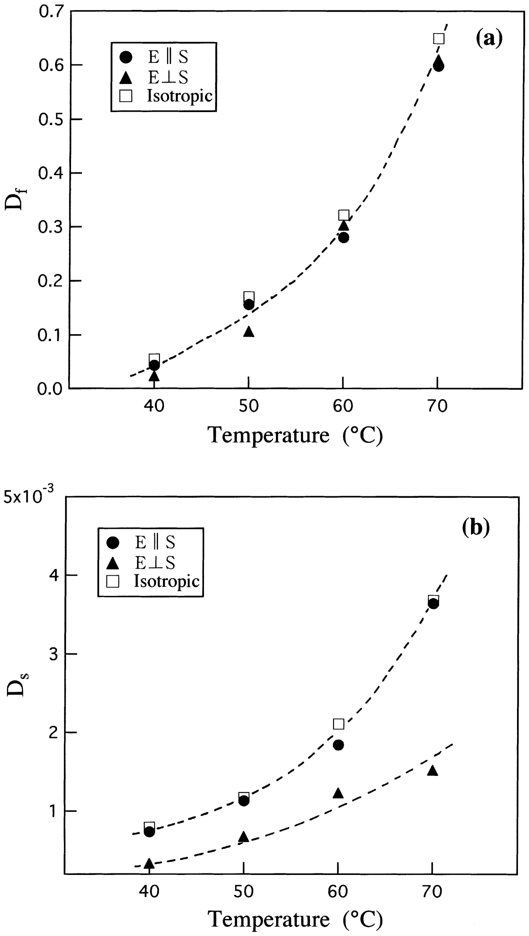

Fig. 9. Temperature dependence of the fast (a) and slow (b) reorientational relaxation rates of HNMA in PMMA films under the three conditions shown in Fig. 8.

[2]. On the other hand, the temperature dependence of the two fractions R_f and R_s of these two relaxation processes is illustrated in Fig. 10. It was found that, the fraction of the slow process gradually decreases whereas the fraction R_f of the fast relaxation component tends to approach unity as the experimental temperature is close to T_g of the PMMA matrix. The results imply that the multiplicity of the relaxation process of HNMA in glassy PMMA tends to disappear upon approaching T_g. Furthermore, the fraction of the fast relaxation process obtained by parallel irradiation is larger than the perpendicular irradiation, revealing the reorientational feasibility of HNMA along the direction parallel to the stretching direction (S).

3.4. Data analysis using the rotational diffusion-controlled reaction model for anisotropic systems

As shown in Fig. 6, though the reaction rate k of the intramolecular photodimerization of HNMA observed along the directions parallel and perpendicular to the stretching direction (S) of the sample increases with increasing tempearure, their difference is not significant. As a consequence,

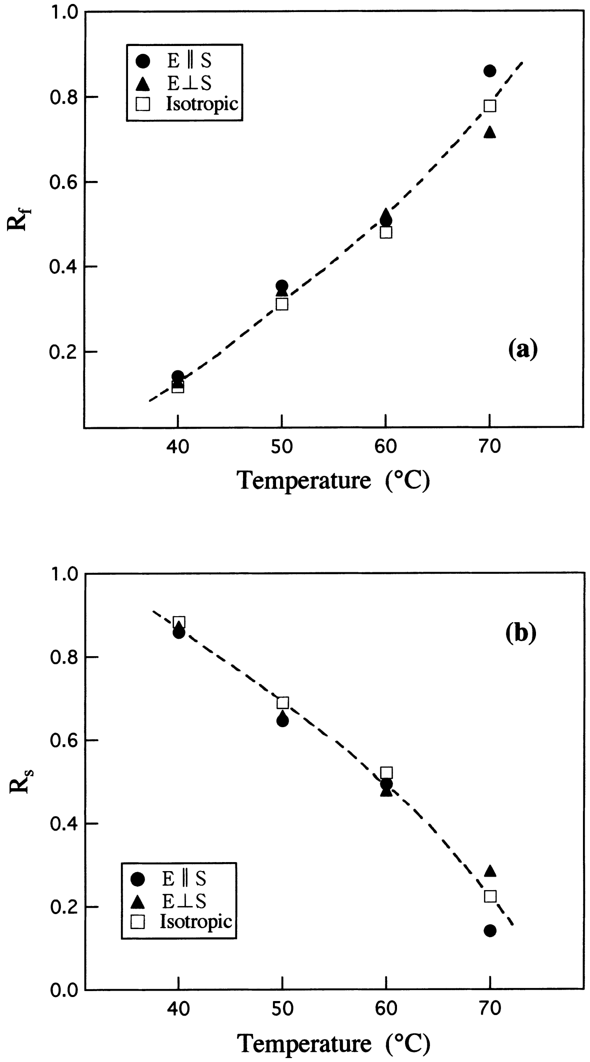

Fig. 10. Temperature dependence of the two fractions R_f and R_s corresponding to the two reorientational relaxation processes shown in Fig. 9.

the temperature dependence of the ratio (*k*/*D*) is determined by the change in the reorientational diffusion coefficient *D*. Shown in Fig. 11 is the temperature dependence of the two ratios k_f/D_f and k_s/D_s observed in the parallel and perpendicular directions with respect to the stretching direction (S). The suffices f and s stand for the fast and slow processes of the reaction kinetics and the reorientational relaxation. From these results, it is obvious that the difference between the transport processes along the parallel and perpendicular directions becomes significant upon decreasing temperature, implying that the data obtained at high temperatures are predominantly affected by the relaxation of polymer chains under uniaxial orientation.

As shown above, the reaction kinetics and the reorientational relaxation of HNMA suggest that there exist in the glassy state of PMMA two distinct environments, the more mobile and the less mobile regions. Provided that the reaction and the reorientational relaxation process of HNMA in these two environments contribute independently to the optical anisotropy of the sample, the total dichroism of HNMA can be written as

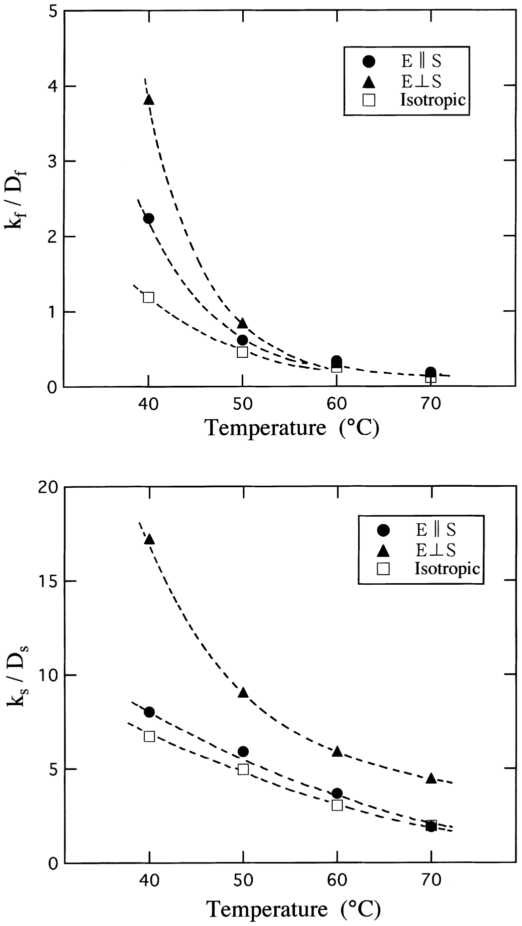

Fig. 11. Temperature dependence of the competition between photo-dimerization and reorientational relaxation of HNMA in PMMA under the three conditions indicated in Fig. 8. Upper part: the fast process; lower part; the slow process.

$$\Delta(t) = F_f\Delta_f(t) + F_s\Delta_s(t) \tag{11}$$

where F_f and F_s are, respectively, the fractional contribution to the dichroism of the sample from HNMA in the less and more mobile regions. According to Eq. (5), the two components Δ_f and Δ_s of the reaction selectivity can be rewritten as

$$\Delta_f(t) = \Delta_{f_{max}}(1 - e^{-t/\tau_f}) \tag{12}$$

and

$$\Delta_s(t) = \Delta_{s_{max}}(1 - e^{-t/\tau_s}) \tag{13}$$

where

$$\Delta_{s_{max}} \cong \frac{1}{(6D_s/k_s) + (1/5)} \tag{14}$$

and

$$\Delta_{f_{max}} \cong \frac{1}{(6D_f/k_f) + (1/5)} \tag{15}$$

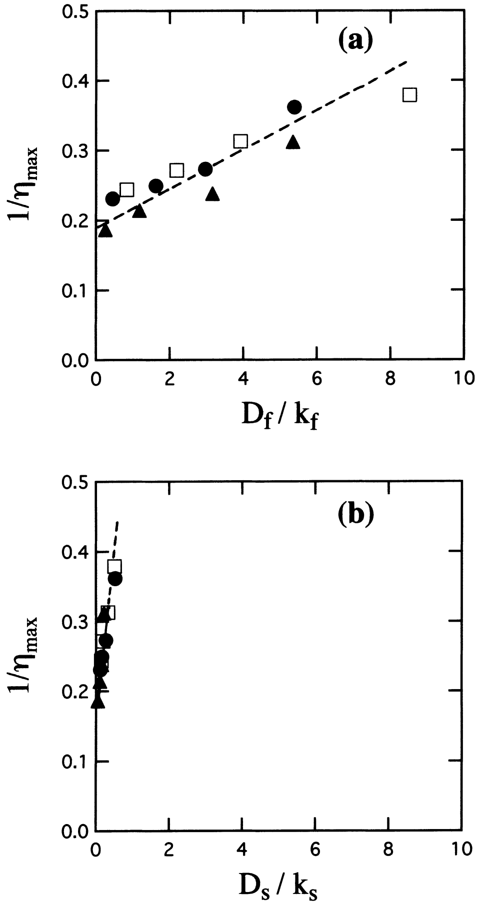

Fig. 12. Correlation between the optical anisotropy generated by linearly polarized light and the reaction-diffusion competition of HNMA in PMMA obtained under three conditions shown in Fig. 8. (a) the fast process; (b) the slow process.

From the kinetic data of the photoisomerization illustrated in Figs. 6 and 7, and the reorientational relaxation data obtained from the annealing-after-irradiation shown in Figs. 9 and 10, it can be concluded that $\Delta_{s_{\max}} \gg \Delta_{f_{\max}}$ over the whole range of temperatures used in this study. In Fig. 12, the inverse of the reaction selectivity ($1/\eta_{\max}$) was plotted versus the ratio (*D*/*f*) for both the fast and the slow processes under the three experimental conditions indicated in Fig. 8. For comparison, these data are plotted on the same scale. Obviously, $1/\eta_{\max}$ exhibits a strong linear dependence on D_s/k_s whereas it varies weakly with (D_f/k_f), suggesting that the maximal magnitude of the dichroism given in Eq. (11) is dominated by the slow component. On the other hand, if the inverse of the characteristic time scale τ in Eq. (7) is defined as

$$\gamma = \frac{1}{\tau} \cong \left(6D + \frac{k}{5}\right) \qquad (16)$$

the inequality $\gamma_s \ll \gamma_f$ holds for the magnitudes of the diffusion coefficient *D* and the reaction rate *k* of the slow and fast processes. As a consequence, the time dependence of the dichroism $\Delta(t)$ or the reaction selectivity $\eta(t)$ is governed by the fast process. This explains the fact that the temporal behavior of $\eta(t)$can be well-expressed by Eq. (5) with a single characteristic time constant τ as shown in Fig. 3.

4. Summary and conclusion

The selectivity of the intramolecular photodimerization of 9-hydroxymethyl-10-{(1-naphthylmethoxy) methyl} anthracene (HNMA) in the glassy region of a uniaxially oriented poly(methyl methacrylate) (PMMA) matrix was investigated by monitoring the reaction kinetics and the reorientational relaxation of the dopant molecule in the directions parallel and perpendicular to the stretching direction of the sample. The effects of the structural anisotropy of the polymer matrix on the photodimerization kinetics of HNMA are not significant because PMMA segments partially undergo reorientational relaxation during the experiments. Neverthless, the following results were obtained for the anisotropic transport process in polymer solid:

1. Intramolecular photodimerization was selected by irradiation with linearly polarized light. The magnitude of the maximum selectivity $\eta_{\max}$ changes in the following order: $\eta_{\max}(\mathrm{E} \perp \mathrm{S}) > (\mathrm{E} \parallel \mathrm{S}) > (\text{isotropic})$. This behavior can be explained by the competition between the reaction and the reorientational relaxation. The time-evolution of the optical anisotropy induced by irradiation with linearly polarized light is dominated by the fast kinetic processes.
2. The reaction kinetics was not significantly affected by the orientation of the sample. Upon approaching the glass transition temperature of the matrix, the fraction of HNMA suppressed in the immobile regions of the glassy PMMA tends to disappear.
3. From the annealing-after-irradiation experiments, it was found that the reorientational relaxation of HNMA is faster along the direction parallel to the stretching direction.
4. The polarization induced photodimerization of HNMA in PMMA can be qualitatively explained by using the rotational diffusion-controlled reaction model proposed recently.

Experiments using HNMA derivatives chemically labeled on polymer chains dispersed in polymer films with larger elongation ratios might provide much more significant characteristics of the anisotropic transport processes in polymer systems. These experiments are underway and their results will be reported later.

Acknowledgements

The financial support from the Ministry of Education, Science and Culture, Japan (Grant-in-Aid No. 11650932) is greatly acknowledged.

References

[1] K. Kinoshita, S. Kawato, A. Ikegami, Biophys. J. 20 (1977) 289.
[2] H.J. Eichler, P. Gunter, D.W. Pohl, Laser-Induced Dynamic Gratings, Springer, Berlin, 1986.
[3] S.A. Jenekhe, K.J. Wynne (Eds.), Photonic and Optoelectronic Polymers, ACS Symposium Series, vol. 672, Am. Chem. Soc., Washington DC, 1995.
[4] Q. Tran-Cong, T. Kumazawa, O. Yano, T. Soen, Macromolecules 23 (1990) 3002.
[5] Q. Tran-Cong, Polarization-induced photochromic reactions in polymer solids, in: J.C. Salamone (Ed.), Polymeric Materials Encyclopedia, vol. 7, CRC Press, Boca Raton, FL, 1996, pp. 5128–5136.
[6] A. Morita, Q. Tran-Cong, Physica A 242 (1997) 377.
[7] Q. Tran-Cong, H. Kanato, S. Chikaki, Polym. Commun. 35 (1994) 4465.
[8] N. Tamura, T. Okamoto, H. Kanato, A. Morita, Q. Tran-Cong, Jpn. J. Polym. Sci. Tech. 55 (1998) 38.
[9] Y. Yamaguchi, T. Okamoto, O. Urakawa, Q. Tran-Cong, Polym. J. 30 (1998) 414.
[10] Y. Imamura, Y. Yamaguchi, Q. Tran-Cong, submitted for publication.
[11] H. Bouas-Laurent, A. Catellan, J.P. Desvergne, Pure Appl. Chem. 52 (1980) 2633.
[12] A. Morita, J. Phys. D 11 (1978) 1357.
[13] Q. Tran-Cong, H. Tanaka, T. Soen, Macromolecules 25 (1992) 7389.
[14] H. Kanato, Q. Tran-Cong, H. Hua, Macromolecules 27 (1994) 7907.
[15] G. Williams, D.C. Watts, Trans. Faraday Soc. 66 (1970) 80.
[16] R. Richert, A. Blumen, Disorder Effects on Relaxational Processes, Springer, Berlin, 1994.
[17] L. Lamarre, C.S.P. Sung, Macromolecules 16 (1983) 1729.
[18] W.C. Yu, C.S.P. Sung, R.E. Robertson, Macromolecules 21 (1988) 355.
[19] J.G. Victor, J.M. Torkelson, Macromolecules 21 (1988) 3490.
[20] I. Mita, K. Horie, K. Hirao, Macromolecules 22 (1989) 558.